

# The Impact of High-Fidelity Model Geometry on Test-Analysis Correlation and FE Model Updating Results

T. Lauwagie<sup>1</sup>, F. Vanhollebeke<sup>2</sup>, B. Pluymers<sup>3</sup>, R. Zegels<sup>4</sup>, P. Verschueren<sup>4</sup>, E. Dascotte<sup>1</sup>

<sup>1</sup>Dynamic Design Solutions NV (DDS)  
Interleuvenlaan 64, B-3001, Leuven, Belgium  
email: [tom.lauwagie@dds.be](mailto:tom.lauwagie@dds.be)

<sup>2</sup>Hansen Transmissions Int. NV  
De Villermontstraat 9, B-2550 Kontich, Belgium

<sup>3</sup>K.U.Leuven, Department Mechanical Engineering  
Celestijnenlaan 300B – box 2420, B-3001 Heverlee, Belgium

<sup>4</sup>Materialise NV  
Technologielaan 15, B-3001, Leuven, Belgium

## Abstract

Structural responses obtained with finite element simulations normally differ from those measured on physical prototypes. In the case of monolithic structures, the differences between the simulated and measured responses are mainly caused by inaccuracies in the geometry and material behavior. The present work focuses on evaluating the impact of using a high-fidelity representation of the actual geometry on the differences between measured and computed resonant frequencies and mode shapes.

This paper presents a study that was performed on a cast-iron lantern housing of a gear box. In a first step, the resonant frequencies and modes shapes of the test structure were measured using impact testing. Next, optical scanning and photogrammetric techniques were used to obtain a 3D virtual point cloud model which accurately describes the surface of the lantern housing. This point cloud was then used to generate a 3D solid finite element model representing the as-built geometry of the housing.

To evaluate the impact of using the actual geometry on the correlation and model updating results, two FE-models were used: an FE-model derived from the measured geometry and an FE-model derived from the CAD model of the lantern housing. Both models have a similar mesh density and mesh quality. These two models were first correlated with the measured modal data and then updated. The geometry appeared to have a significant impact on both the correlation and updating results.

## 1 Introduction

Structural responses obtained with finite element simulations normally differ from those measured on physical prototypes. The observed differences are mainly caused by inaccuracies in the geometry, material behavior and joint properties of the simulation model. Finite element model updating [1] is a commonly accepted technique to improve the validity of simulation models. By tuning physical element properties, model updating aims at reducing the differences between the measured and simulated responses as much as possible. However, in the case of 3D solid elements, the geometry of the model is not controlled by element properties, like a shell thickness in the case of 2D elements, but by the positions of the nodes of the elements. Direct updating of the individual nodal positions would lead to an excessive amount of independent updating variables and is therefore practically unfeasible. With 3D elements, the geometrical uncertainties are usually compensated in an indirect way. For example, an overestimation of a thickness has to be compensated by a reduction of the stiffness and mass density of the material in the

considered component. Although such compensations can eventually provide models that correlate well with the test data set, the improvement in reliability of the model is limited as the modifications are physically not correct, which restricts the application range of the updated finite element model.

The goal of the present work was to investigate the impact of the geometrical inaccuracies on the correlation between numerical and experimental resonant frequencies and mode shapes. To simplify matters, a monolithic cast-iron lantern housing was used. In this way the impact of uncertainties any joint properties was eliminated. A high-fidelity representation of the geometry was obtained by a combination of optical scanning and photogrammetry. The point cloud that resulted from these optical measurements served as a starting point to generate a 3D solid finite element model representing the as-built geometry of the housing.

To evaluate the impact of using the actual geometry on the correlation and model updating results, two FE-models were used: an FE-model derived from the measured geometry and an FE-model derived from the CAD model of the lantern housing. Both models had a similar mesh density and mesh quality. These two models were first correlated with the measured modal data and then updated.

## 2 Measuring the Geometry

To obtain an accurate geometrical description of the lantern housing, optical scanning and photogrammetric techniques were used to acquire a point cloud of the part as-built. Optical scanning was performed using a GOM ATOS I scanner, shown in Figure 1.



**Figure 1: GOM ATOS I scanner which was used to digitize the lantern housing.**

The digitizing principle is based on a white light fringe pattern from a projector (center part on Figure 1) onto the scanned object. Two cameras (left and right on Figure 1) capture images of the object and reference geometries. Since the lantern housing is too large to fit the scanning volume of the ATOS I scanner, photogrammetric techniques were applied by using the ATOS TRITOP system. Photogrammetry uses photographic images of multiple marker systems to allow the ATOS software to merge optical scans of different regions of the lantern housing. Figure 2 shows pictures of the lantern housing during the scanning process. A white spray is applied to reduce reflections. Small marker stickers are used for local optical scanning. Large stickers and two reference bars on the ground are used for the TRITOP imaging.

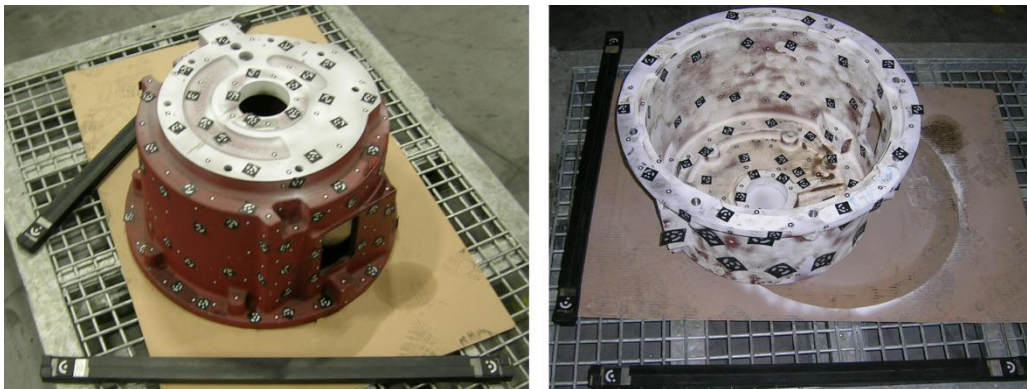


**Figure 2: Images showing the lantern housing during the digitizing process.**

Triangulation techniques are applied to reconstruct a point cloud from these images based on the distance and angle between the cameras, the projected grid information and the photogrammetry pictures. Using the GOM ATOS Professional software [2] the point cloud data is converted into the Standard Triangulation Language (STL) model shown in Figure 3. An STL model is a triangle facet surface mesh representation based on the scanned point cloud. In case of the lantern housing, the minimal geometrical accuracy of this STL model, taking into account scanning and point cloud post-processing, is approximately 0.2 mm. This model still contains imperfections such as missing edges and unscannable areas like holes. The post-processing procedure to resolve these issues is discussed in the next paragraph.

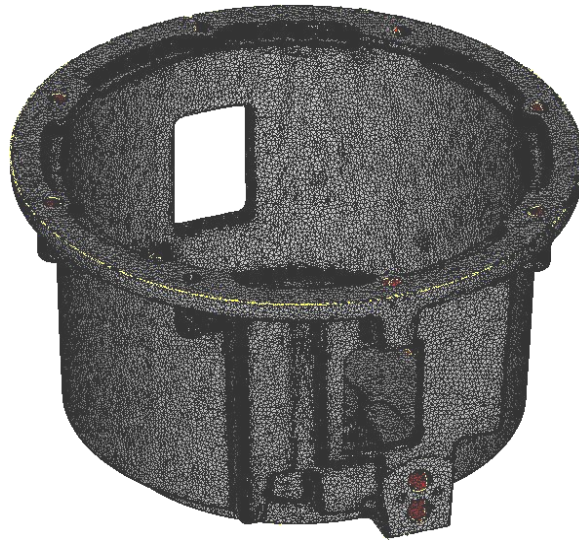


**Figure 3: STL triangle mesh model resulting from the digitizing process.**

### **3 STL Fixing and Finite Element Meshing**

The STL model resulting from the digitization process is not suitable to generate an FE mesh because it is not watertight, as shown in Figure 4. Furthermore, the mesh density and quality of the STL model are not appropriate for FE analysis. Therefore, the model is imported into the STL fixing, design & meshing software package 3-matic from Materialise [3].

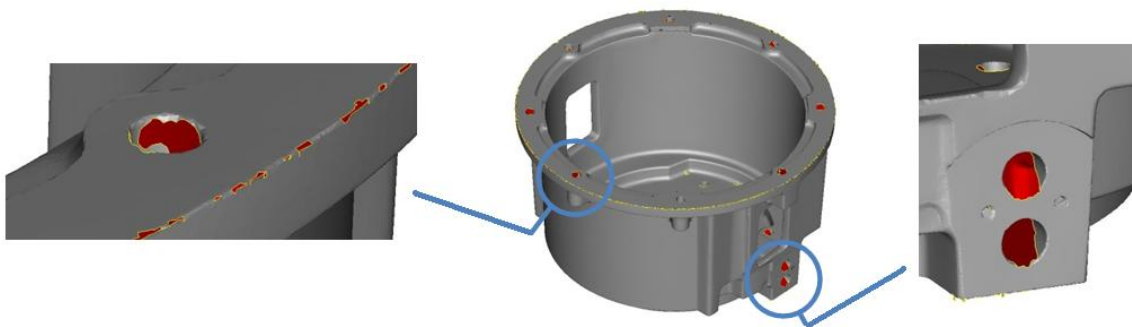


**Figure 4: Detail views of typical scan surface mesh imperfections: non-watertight edges (left) and incomplete hole or slot information (left and right).**

For the virtual fixing of slots and holes CAD information was locally copied into the scan to complete the missing geometry. This is justified since all holes and slots are CNC drilled independent from the cast geometry for reasons of alignment. The defects along the edges were fixed using automated hole filling algorithms.

Once the model was watertight, the mesh was optimized in the 3-matic Remesh module. An element quality histogram was used to drive the automatic remeshing procedure, as shown in Figure 5. Before the remeshing procedure, the STL model coming from scan contained 432757 triangles. Normalized element skewness of the worst element was smaller than 0.005. This implies that the model comprises highly skewed elements which lead to mathematical instabilities during FEA solving. The remeshing procedure, which allowed for a maximum local deformation of the model of 0.5 mm, reduced the number of triangles to 30976. The minimal normalized element skewness was increased up to 0.35.

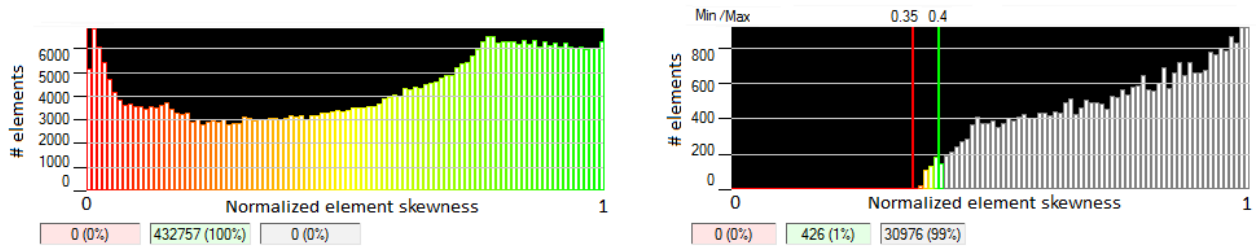


**Figure 5: Histograms showing the triangle element quality before (left) and after (right) the automated remeshing procedure in 3-matic.**

From the optimized surface mesh a 10-noded tetrahedron volume mesh with 54040 elements was generated. The elements had a minimal equi-angle skewness of 0.11, providing a mathematically stable FE mesh. A section of the final volume mesh is shown in Figure 6.

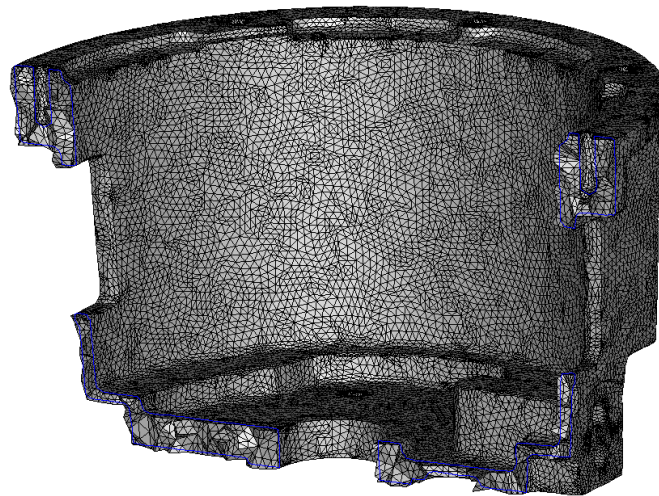


**Figure 6: Resulting 10-noded tetrahedron mesh containing 54040 elements.**

## 4 Experimental Modal Analysis

### 4.1 Experimental Set-up

The goal of the experimental modal analysis is to measure the resonant frequencies and mode shapes up to 1.5 kHz. The test structure was suspended with a number of elastic bands as shown in Figure 7. The Frequency Response Functions (FRFs) are measured using a roving hammer test (PCB – 086C03) and using 6 tri-axial accelerometers (PCB – 356A15). The input and response signal are measured up to 2 kHz using 2048 spectral lines, which results in a measurement time of 1 s. To minimize the impact of noise and leakage, a hammer window (1%) was used on the input signals and an exponential window (10%) was used on the responses signals. The average of 5 individual FRFs measurements is used as

measured FRF. The measurements were performed at the K.U.Leuven using a Scadas III data acquisition system and the LMS Test.Lab modal analysis software [7].

The FEMtools [4] modal pretest analysis module was used to find the optimal excitation and measurement locations. Based on the results of the pretest analysis 38 measurements points were selected: 16 points along the edge of the top surface, 16 point in the middle of the side surface and 6 points on the bottom surface. On the top surface points, the structure was excited in the radial and vertical direction. On the side surface, the structure was excited in the radial direction only while on the bottom surface the structure was only excited in the vertical direction. Of the 6 tri-axial accelerometers, 3 were placed on the top surface, 2 were placed on the side surface, and 1 was placed on the bottom surface.

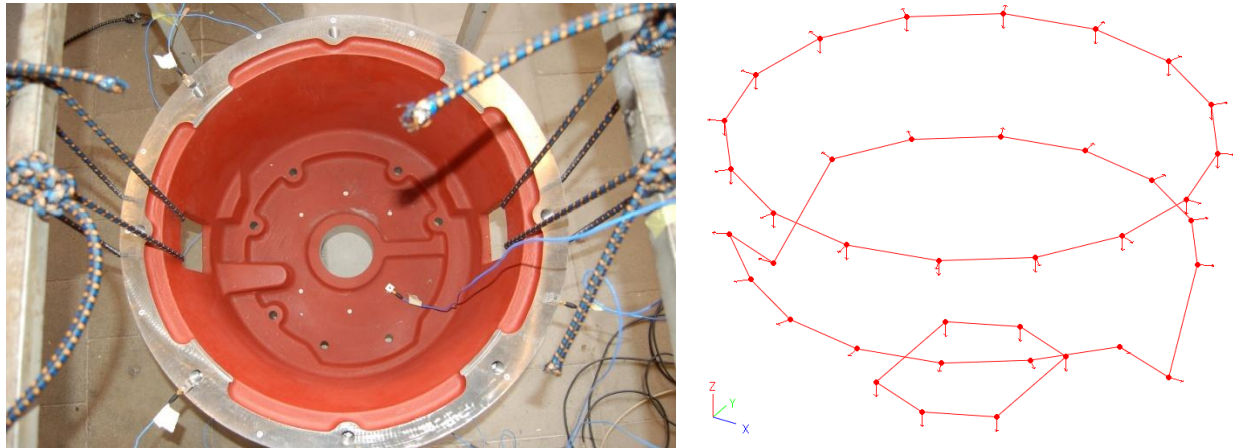


**Figure 7: The test set-up (left) and the measurement DOFs (right).**

## 4.2 Modal Parameter Estimation

Using the p-LSCFD [6] modal parameter estimator, eighteen stable modes could be extracted from the measured FRFs in the frequency range of interest. Table 1 gives an overview of the identified modal parameters. Figure 8 shows the auto-MAC matrix between the identified test modes. All off-diagonal values are smaller than 15%.

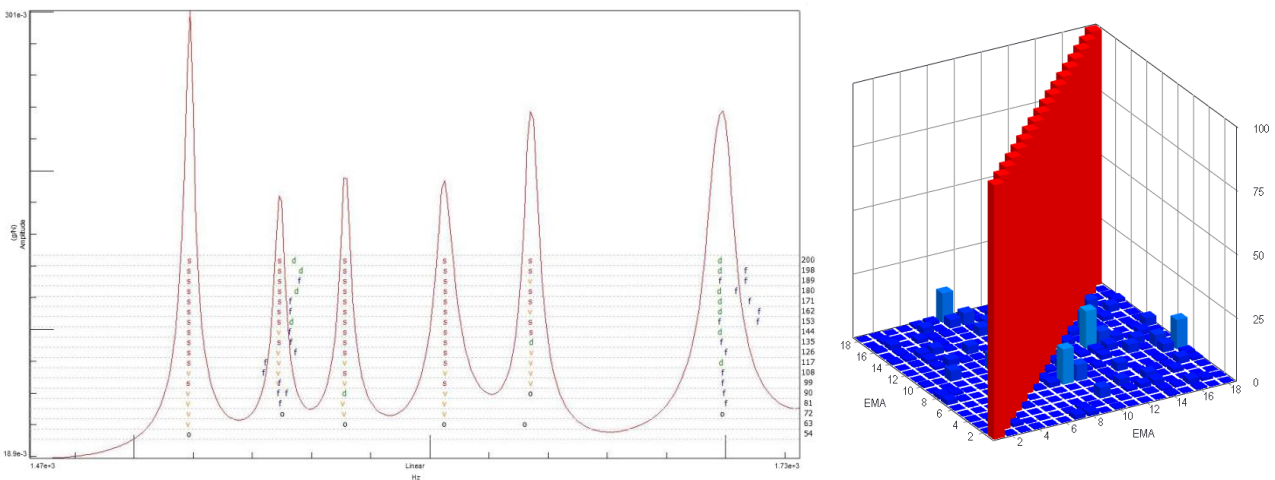


**Figure 8: Stabilization diagram of a section of the examined frequency band (left) and the autoMAC of the identified mode shapes (right).**

Mode	Frequency [%]	Damp. ratio [%]	Mode	Frequency [%]	Damp. Ratio [%]
1	262.614	0.04	10	1298.113	0.08
2	264.713	0.01	11	1347.696	0.08
3	649.294	0.03	12	1369.621	0.16
4	710.809	0.05	13	1383.928	0.18
5	737.190	0.06	14	1417.953	0.08
6	1058.836	0.09	15	1518.864	0.08
7	1079.801	0.08	16	1548.991	0.17
8	1097.152	0.11	17	1570.844	0.12
9	1102.419	0.11	18	1604.823	0.16

**Table 1: The experimental modal parameters.**

## 5 Evaluation of the Impact of the Measured Geometry

The impact of using high-fidelity geometries was evaluated by comparing the reliability of the responses of the CAD-based model with those of the geometry-based model. Both FE-models had similar number of elements ( $\pm 55000$ ) to exclude the influence of the mesh density.

The correlation analysis was performed twice. The first time the modal parameters of the FE-models were compared with the experimental modal parameters. The second time, the FE-models were first updated and the correlation analysis was performed using the updated FE-models.

### 5.1 Initial Correlation

#### 5.1.1 The CAD-Based FE-Model

The correlation analysis between the results of the CAD-based FE-modal and the test provided 18 mode shape pairs. The mode shape order in the two data sets was identical. The correlation results show that the FE-model underestimated all the frequency about 6.9 %. The MAC values ranged between 40.1 and 97.7, with an average value of 82.0. Table 2 provides a detailed overview of the correlation results for the frequencies and mode shapes.

Pair	FEA	Freq. [Hz]	EMA	Freq. [Hz]	Diff. [%]	MAC
1	1	243.26	1	262.61	-7.37	89.0
2	2	245.50	2	264.71	-7.26	87.8
3	3	589.48	3	649.29	-7.83	93.6
4	4	661.47	4	710.81	-6.94	86.3
5	5	997.62	5	737.19	-3.68	83.6
6	6	1003.7	7	1079.8	-7.61	92.8
7	7	1012.1	8	1097.2	-8.52	40.1
8	8	1060.7	6	1058.8	-4.41	43.2
9	9	1060.7	9	1102.4	-3.78	72.6
10	10	1202.1	10	1298.1	-7.40	88.7
11	11	1256.9	11	1347.7	-6.74	97.7
12	12	1267.0	12	1369.6	-7.49	86.3
...						

13	13	1280.0	13	1383.9	-7.51	85.1
14	14	1308.2	14	1418.0	-7.74	94.4
15	15	1410.5	15	1518.9	-7.14	96.4
16	16	1437.9	16	1549.0	-7.17	80.0
17	17	1451.6	17	1570.8	-7.59	77.1
18	18	1483.3	18	1604.8	-7.57	81.3

**Table 2: Correlation between CAD-based FE-model and the test results.**

### 5.1.2 The Geometry-Based FE-Model

The correlation analysis between the results of the geometry-based FE-model and the test also provided 18 mode shape pairs. As for the CAD-based model, the order of the FE-modes corresponded with the order of the test modes. The correlation results show that the geometry based FE-model underestimated all the resonance frequency about 8.6 %. The MAC values ranged between 88.8 and 97.8, with an average value of 83.8. Table 3 provides a detailed overview of the correlation results for the frequencies and mode shapes.

Pair	FEA	Freq. [Hz]	EMA	Freq. [Hz]	Diff. [%]	MAC
1	1	240.21	1	262.61	-8.53	91.1
2	2	241.93	2	264.71	-8.61	88.8
3	3	593.25	3	649.29	-8.63	93.6
4	4	650.55	4	710.81	-8.48	96.9
5	5	674.79	5	737.19	-8.46	96.8
6	6	966.37	7	1058.8	-8.73	97.8
7	7	989.01	8	1079.8	-8.41	97.8
8	8	1001.2	6	1097.2	-8.75	89.4
9	9	1007.9	9	1102.4	-8.58	89.4
10	10	1184.0	10	1298.1	-8.79	88.9
11	11	1227.8	11	1347.7	-8.90	96.6
12	12	1250.1	12	1369.6	-8.73	93.8
13	13	1265.9	13	1383.9	-8.53	93.3
14	14	1292.0	14	1418.0	-8.88	97.1
15	15	1386.5	15	1518.9	-8.72	97.1
16	16	1418.2	16	1549.0	-8.44	91.2
17	17	1436.8	17	1570.8	-8.53	93.3
18	18	1466.0	18	1604.8	-8.65	95.5

**Table 3: Correlation between the geometry-based FE-model and the test results.**

## 5.2 Model Updating

The FE-models were updated using the FEMtools [4] model updating module. The updating procedure that was used consisted of two separate steps. In the first step the overall mass of the FE-model was set to the mass value of the test structure by modifying the mass density of the material in the model. In the second step the stiffness of the model was updated by modifying the Young's modulus of the FE-model. The Young's modulus was defined as a global parameter, i.e. the Young's modulus remained uniform over the whole FE-model during updating. The 18 measured resonant frequencies were used as targets for

the updating procedure. The mode shape data was only used for mode tracking purposes, not as target values for the updating.

### 5.2.1 The CAD-Based FE-Model

The CAD-based FE-model underestimated the mass by 3 kg, i.e. 108.0 kg instead of 111.0 kg. To increase the mass by 3 kg, the mass density of the material had to be raised from 7100 to 7295 kg/m<sup>3</sup>. The mass correction resulted in a drop of the overall frequency correlation with 1.2 %, i.e. -8.1 % instead of -6.9%.

The stiffness updating of the FE-model increased the Young's modulus from 110.5 GPa to 130.7 GPa. This resulted in frequency residuals between -1.72 % and 3.64. Note that a global updating of the mass and stiffness does not have a significant effect on the mode shapes. Hence, the updating does not provide any improvement in the mode shape correlation.

Pair	FEA	Freq. [Hz]	EMA	Freq. [Hz]	Diff. [%]	MAC
1	1	261.48	1	262.61	-0.43	89.0
2	2	263.77	2	264.71	-0.36	87.8
3	3	643.63	3	649.29	-0.87	93.6
4	4	710.75	4	710.81	-0.01	86.3
5	5	764.00	5	737.19	3.64	83.6
6	6	1073.6	6	1058.8	-0.58	92.8
7	7	1078.3	7	1079.8	-1.72	40.1
8	8	1085.9	8	1097.2	2.56	43.2
9	9	1139.6	9	1102.4	3.37	72.6
10	10	1290.3	10	1298.1	-0.61	88.7
11	11	1346.7	11	1347.7	-0.07	97.7
12	12	1361.2	12	1369.6	-0.61	86.3
13	13	1375.7	13	1383.9	-0.60	85.1
14	14	1402.4	14	1418.0	-1.10	94.4
15	15	1510.0	15	1518.9	-0.58	96.4
16	16	1547.3	16	1549.0	-0.11	80.0
17	17	1558.9	17	1570.8	-0.76	77.1
18	18	1592.4	18	1604.8	-0.77	81.3

**Table 4: The correlation between the updated CAD-based FE-model and the test results.**

### 5.2.2 The Geometry-Based FE-Model

The geometry-based FE-model had an overall mass of 105.0 kg instead of the 111.0 kg of the test model. This required an increase of the mass density of the material from 7100 kg/m<sup>3</sup> to 7503 kg/m<sup>3</sup>. This increase resulted in an overall frequency drop of 2.5 %; increasing the underestimation of the resonant frequencies by the FE-model.

The second step of the updating procedure increased the Young's modulus from 110.5 GPa to 139.9 GPa resulting in frequency residuals between -0.29 % and 0.24 %.

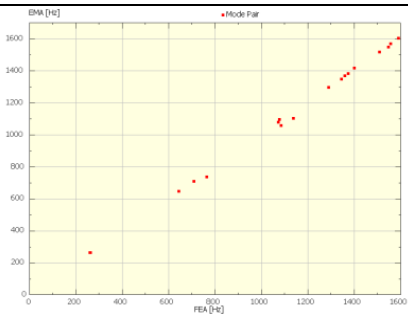
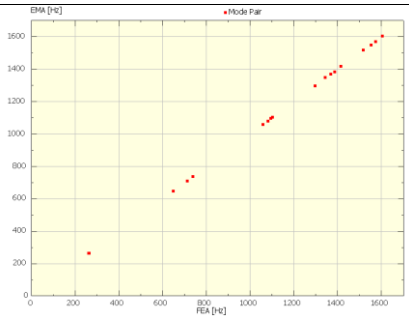


Pair	FEA	Freq. [Hz]	EMA	Freq. [Hz]	Diff. [%]	MAC
1	1	262.90	1	262.61	0.11	91.1
2	2	264.78	2	264.71	0.03	88.9
3	3	649.29	3	649.29	0.00	93.7
4	4	712.00	4	710.81	0.17	96.8
5	5	738.53	5	737.19	0.18	97.1
6	6	1057.7	6	1058.8	-0.11	97.8
7	7	1082.4	7	1079.8	0.24	98.2
8	8	1095.8	8	1097.2	-0.13	90.6
9	9	1103.1	9	1102.4	0.06	90.1
10	10	1295.9	10	1298.1	-0.17	89.5
11	11	1343.7	11	1347.7	-0.29	98.2
12	12	1368.1	12	1369.6	-0.11	94.2
13	13	1385.5	13	1383.9	0.11	93.2
14	14	1414.0	14	1418.0	-0.28	97.3
15	15	1517.4	15	1518.9	-0.10	97.2
16	16	1552.2	16	1549.0	0.20	93.0
17	17	1572.5	17	1570.8	0.11	95.5
18	18	1604.5	18	1604.8	-0.02	95.0

**Table 5: The correlation between the updated geometry-based FE-model and the test results.**

### 5.3 Comparison

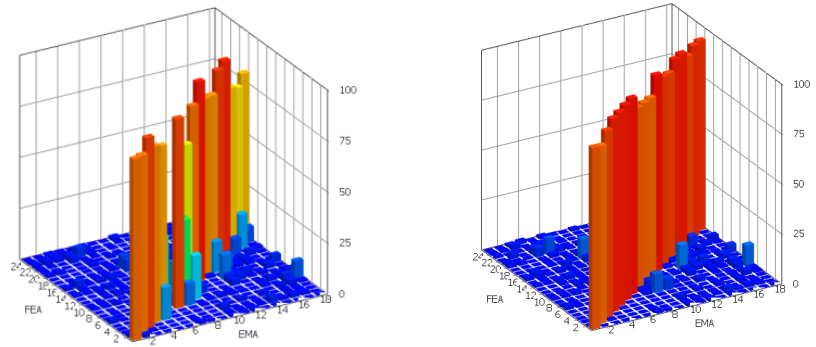
Table 6 provides an overview between the correlation results of the update CAD-based FE-model and the updated geometry-based FE-model with the measured mode shapes and resonant frequencies. The frequency match of the updated geometry-based FE-model is significantly better than the frequency match of the CAD-based FE-model. However, the most remarkable difference between the two models is their correlation with the test modes. While the CAD-based FE-model is missing a few mode shape pairs, the geometry based FE-model has an excellent correlation for all 18 considered modes.

	CAD-based FE-model	Geometry-based FE-model
Frequency residuals		
Average [freq. residual]	1.04%	0.14%
Min. [freq. residual]	0.01%	0.00%
Max. [freq. residual]	3.64%	0.29%

...

---

## MAC FEM-EMA



Average MAC	82.0	94.3
Minimum MAC	40.1	88.9
Maximum MAC	97.7	98.2
Updated mass density	7295 kg/m <sup>3</sup>	7503 kg/m <sup>3</sup>
Updating young's modulus	130.7 GPa	139.9 GPa

---

**Table 6: Comparison of the CAD-based and geometry-based FE-model.**

## 6 Conclusions

The presented work evaluates the impact of using a high-fidelity representation of the geometry of a monolithic cast-iron structure on the correlation between measured and simulated responses. The use of the as-built geometry of the structure, obtained by optical scanning of a prototype, provides a significant improvement in the correlation between the measured and simulated mode shapes in a wide frequency range. As such, the use of the as-built geometry eliminates, or at least reduces, the need of equivalent parameter changes to compensate the effects of geometrical inaccuracies. As the updating process provides parameter changes that are physically more relevant, the application range in which the updated FE-model can be used as a reliable predictive tool for design optimization can be increased.

## Acknowledgements

The authors would like to thank Kristof Marcelis, Carl Moerman and Tobe Possemiers for performing the experimental modal analysis.

## References

- [1] E. Dascotte, *Model Updating for Structural Dynamics: Past, Present and Future Outlook*. In proceedings of the International Conference on Engineering Dynamics (ICED), April 16-18, 2007, Carvoeiro, Algarve, Portugal.
- [2] GOM ATOS Professional Software Manual, 2010
- [3] Materialise, 3-matic 5.0 manual, 2010
- [4] FEMtools, [www.femtools.com](http://www.femtools.com)
- [5] W. Heylen, S. Lammens, P. Sas, *Modal Analysis Theory and Testing*, Katholieke Universiteit Leuven, Departement Werktuigkunde, Leuven (1997)
- [6] K. Marcelis, C. Moerman, T. Possemiers, *Structuurdynamica: analyse en numerieke modellering. Modale analyse van een tandwielkast*, Katholieke Universiteit Leuven, Departement Werktuigkunde, Leuven, 2010. (Internal K.U.Leuven document)
- [7] LMS Test.Lab, [www.lmsintl.com](http://www.lmsintl.com)